0026-895X/09/7501-242–253$20.00
MOLECULAR PHARMACOLOGY
Vol. 75, No. 1
51128/3423242
Mol Pharmacol 75:242–253, 2009
Printed in U.S.A.

Inhibition of Arachidonic Acid and Iron-Induced Mitochondrial Dysfunction and Apoptosis by Oltipraz and Novel 1,2-Dithiole-3-thione Congeners

Sang Mi Shin and Sang Geon Kim

Innovative Drug Research Center for Metabolic and Inflammatory Diseases, College of Pharmacy and Research Institute of Pharmaceutical Sciences, Seoul National University, Seoul, Korea

Received August 5, 2008; accepted October 21, 2008

ABSTRACT

4-Methyl-5-(2-pyrazinyl)-1,2-dithiole-3-thione (oltipraz), a prototype drug candidate containing a 1,2-dithiole-3-thione moiety, has been widely studied as a cancer chemopreventive agent. Oltipraz and other novel 1,2-dithiole-3-thione congeners have the capability to prevent insulin resistance via AMP-activated protein kinase (AMPK) activation. Arachidonic acid (AA, a proinflammatory fatty acid) exerts a deleterious effect on mitochondria and promotes reactive oxygen species (ROS) production. This study investigated whether AA alone or in combination with iron (catalyst of autooxidation) causes ROS-mediated mitochondrial impairment, and if so, whether oltipraz and synthetic 1,2-dithiole-3-thiones protect mitochondria and cells against excess ROS produced by AA + iron. Oltipraz treatment effectively inhibited mitochondrial permeability transition promoted by AA + iron in HepG2 cells, thereby protecting cells from ROS-induced apoptosis. Oltipraz was found to attenuate apoptosis induced by rotenone (complex I inhibitor), but not that by antimycin A (complex III inhibitor), suggesting that the inhibition of AA-induced apoptosis by oltipraz might be associated with the electron transport system. AMPK activation by oltipraz contributed to cell survival, which was supported by the reversal of oltipraz's restoration of mitochondrial membrane potential by concomitant treatment of compound C. By the same token, an AMPK activator inhibited AA + iron-induced mitochondrial permeability transition with an increase in cell viability. Moreover, new 1,2-dithiole-3-thiones with the capability of AMPK activation protected cells from mitochondrial permeability transition and ROS overproduction induced by AA + iron. Our results demonstrate that oltipraz and new 1,2-dithiole-3-thiones are capable of protecting cells from AA + iron-induced ROS production and mitochondrial dysfunction, which may be associated with AMPK activation.

4-Methyl-5-(2-pyrazinyl)-1,2-dithiole-3-thione (oltipraz), a prototype drug candidate containing a 1,2-dithiole-3-thione moiety, has been widely studied as a cancer chemopreventive agent (Bolton et al., 1993; Jacobson et al., 1997; Wang et al., 1999; Kang et al., 2003). Oltipraz has also been studied in the treatment of liver cirrhosis (Kang et al., 2002). Studies from this laboratory and others indicated that the cancer chemopreventive properties of oltipraz might be associated with the phosphatidylinositol 3-kinase-dependent activation of CCAAT/enhancer binding protein and the consequent changes in target gene transactivation (e.g., phase II antioxidant enzymes) (Kensler, 1997; Kang et al., 2003). More recently, oltipraz and other novel 1,2-dithiole-3-thione congeners were found to have the capability to prevent insulin resistance induced by tumor necrosis factor-α (TNFα) (Bae et al., 2007), a cytokine that promotes the production of reactive oxygen species (ROS) (Xue et al., 2005). The signaling pathway responsible for the restoration of insulin sensitivity may involve AMP-activated protein kinase (AMPK) (Bae et al., 2007).

The mitochondrial respiratory chain is a major source of ROS under pathological conditions (Browning and Horton, 2004). Oxidative stress is therefore implicated in cell injury, thereby causing inflammatory processes (Browning and Hor-

This work was supported by the Korea Science and Engineering Foundation (KOSEF) funded by the government (MEST) [Grant R11-2007-107-01001-0].
Article, publication date, and citation information can be found at http://molpharm.aspetjournals.org.
doi:10.1124/mol.108.051128.

ABBREVIATIONS: TNFα, tumor necrosis factor-α; ROS, reactive oxygen species; AMPK, AMP-activated protein kinase; AA, arachidonic acid; ACC, acetyl-CoA carboxylase; PARP, poly(ADP-ribose)polymerase; NTA, nitrilotriacetic acid; AICAR, 5-aminoimidazole-4-carboxamide-1-β-D-ribofuranoside; MTT, 3-(4,5-dimethylthiazol-2-yl)-2,5-diphenyl-tetrazolium bromide; Rh123, rhodamine 123; PI, propidium iodide; DCFH-DA, 2′, 7′-dichlorofluorescin diacetate; PEG-SOD, polyethylene glycol-superoxide dismutase; NAC, *N*-acetyl-L-cysteine; MMP, mitochondrial membrane potential; S6K1, p70 ribosomal S6 kinase-1; GSK3β, glycogen synthase kinase-3β; MEM, minimal essential medium; PBS, phosphate-buffered saline; ER, endoplasmic reticulum; CHOP, CCAAT enhancer-binding protein homologous protein; Grp78, glucose-regulated protein 78; TUNEL, terminal deoxynucleotidyl transferase dUTP nick-end labeling.

ton, 2004). It is well recognized that oxidative stress causes the modification of membrane phospholipids. Oxidative modification of fatty acids and phospholipids may detrimentally affect cell signaling. In response to ROS and proinflammatory cytokines, oxidized fatty acids, which are esterified in phospholipids, may activate phospholipases (Balboa and Balsinde, 2006). As a result, lipid peroxidation in cells may promote the release of arachidonic acid (AA), a biologically active proinflammatory mediator (Balboa and Balsinde, 2006).

AA, an ω-6 polyunsaturated fatty acid, mediates oxidative stress and inflammation. Indeed, a marked enhancement in the ratio of ω-6/ω-3 fatty acids occurs in patients with cardiovascular disease, cancer, and hepatitis (Araya et al., 2004; Dwyer et al., 2004; Simopoulos, 2006). AA produced as a consequence of oxidative stress is used for the production of proapoptotic prostaglandins or leukotrienes (Neale et al., 1988; Chang et al., 1992). Furthermore, AA can directly activate sphingomyelinase, which catalyzes the production of proapoptotic ceramide (Jayadev et al., 1994). Ceramide can then alternatively propagate apoptotic signals. Moreover, AA releases Ca^{2+} from intracellular stores and increases Ca^{2+} uptake into mitochondria, which may lead to apoptosis (Scorrano et al., 2003). Moreover, studies have indicated that AA exerts a direct effect on mitochondria and promotes ROS production (Cocco et al., 1999; Scorrano et al., 2001).

Iron overload is common in inflammatory conditions such as chronic hepatitis and ethanol ingestion (Valerio et al., 1996; George et al., 1998), which increases oxidant production, lipid peroxidation, protein oxidation, and DNA damage. It is well known that iron is a catalyst of autooxidation. Moreover, iron may cause the release of AA by oxidative modification of membrane phospholipids, enhancing oxidative stress and inflammation (Tadolini and Hakim, 1996; Mattera et al., 2001). Hence, AA and iron synergistically increase oxidative stress and cell death (Caro and Cederbaum, 2001). In the present study, the hypothesis that AA and iron catalyze the overproduction of ROS and induce mitochondrial dysfunction leading to cell death was tested.

Despite the extensive studies on oltipraz's effects on phase II enzyme induction, whether oltipraz as a chemopreventive agent has a direct cytoprotective effect against excess ROS has not been explored. In this regard, this study investigated whether oltipraz and novel 1,2-dithiole-3-thione congeners inhibit mitochondrial dysfunction and cell death induced by AA + iron. In particular, whether 1,2-dithiole-3-thiones with the ability to activate AMPK protect cells from mitochondrial impairment and resultant ROS production was examined. Data showing that a novel class of 1,2-dithiole-3-thiones exerted cytoprotective effects against AA + iron through AMPK-dependent inhibition of mitochondrial impairment, and ROS production would provide insight into free radical-mediated biological processes and possible strategies for chemical intervention.

Materials and Methods

Materials. Oltipraz was provided from CJ Corporation (Seoul, Korea). 1,2-Dithiole-3-thione compounds were synthesized at CJ Central Laboratories (Ichon City, Korea) as described previously (Bae et al., 2007, 2008). MitoSOX was obtained from Molecular Probes (Carlsbad, CA). Anti-procaspase-3, anti-phospho-acetyl-CoA carboxylase (ACC), anti-phospho-AMPK, and anti-AMPK antibodies were supplied from Cell Signaling Technology (Danvers, MA). Antibodies directed against poly(ADP-ribose)polymerase (PARP) and Bcl-x_L were purchased from Santa Cruz Biotechnology (Santa Cruz, CA). Horseradish peroxidase-conjugated goat anti-rabbit and goat anti-mouse IgGs were provided from Zymed Laboratories (San Francisco, CA). Compound C was purchased from Calbiochem (Darmstadt, Germany). DeadEnd Colorimetric TUNEL System was obtained from Promega (Madison, WI). AA, ferric nitrate, nitrilotriacetic acid (NTA), 5-aminoimidazole-4-carboxamide-1-β-D-ribofuranoside (AICAR), 3-(4,5-dimethylthiazol-2-yl)-2,5-diphenyltetrazolium bromide (MTT), rhodamine-123 (Rh123), propodium iodide (PI), 2′,7′-dichlorofluorescin diacetate (DCFH-DA), anti-β-actin antibody, polyethylene glycol-superoxide dismutase (PEG-SOD), PEG-catalase, Trolox, *N*-acetyl-L-cysteine (NAC), and other reagents were supplied from Sigma (St. Louis, MO). The solution of iron-NTA complex was prepared as described previously (Sakurai and Cederbaum, 1998). In brief, equal volumes of 50 mM ferric nitrate in 1 N HCl and 150 mM NTA in 1 N NaOH solution were mixed immediately before the assay, and the pH of the solution was adjusted to 7.4 with $NaHCO_3$ solution.

Cell Culture and Treatment. HepG2 cells, a human hepatocyte-derived cell line, were supplied from American Type Culture Collection (Manassas, VA) and maintained in Dulbecco's modified Eagle's medium containing 10% fetal bovine serum, 50 U/ml penicillin, and 50 μg/ml streptomycin at 37°C in humidified atmosphere with 5% CO_2. For all experiments, cells (1×10^6) were plated in a 10-cm^2 plastic dish for 2 to 3 days (i.e., 80% confluence) and serum-starved for 24 h. The cells were incubated with 3 to 30 μM AA for the time period indicated under *Results* or in the figure legends. For combinatorial treatments with iron, the cells were treated with AA for 12 h, washed with minimum essential medium (MEM), and then incubated with iron. To assess the effects of oltipraz, the cells were treated with 1 to 60 μM oltipraz for 30 min before incubation with AA or AA + iron. In other experiments, the cells were treated with 30 μM each of the 1,2-dithiole-3-thiones or 500 to 1000 μM AICAR and continuously exposed to AA or AA + iron.

MTT Cell Viability Assay. HepG2 cells were plated at a density of 5×10^4 cells/well in a 96-well plate to measure cytotoxicity. After treatment, viable cells were stained with MTT (0.25 mg/ml, 4 h). The media were then removed and formazan crystals produced in the wells were dissolved by the addition of 200 μl of dimethyl sulfoxide. Absorbance was measured at 540 nm using an enzyme-linked immunosorbent assay microplate reader (Tecan, Research Triangle Park, NC). Cell viability was defined relative to untreated control [i.e., viability (percentage of control) = 100 × (absorbance of treated sample)/(absorbance of control)].

TUNEL Assay. TUNEL assay was performed using a commercially available kit, DeadEnd Colorimetric TUNEL System (Promega), according to the manufacturer's instructions. HepG2 cells were fixed with 10% buffered formalin in PBS at room temperature for 30 min and permeabilized with 0.2% Triton X-100 for 5 min. After washing with PBS, each sample was incubated with biotinylated nucleotide and terminal deoxynucleotidyltransferase in 100 μl of equilibration buffer at 37°C for 1 h. The reaction was stopped by immersing the samples in 2× saline sodium citrate buffer for 15 min. Endogenous peroxidases were blocked by immersing the samples in 0.3% H_2O_2 for 5 min. The samples were treated with 100 μl of horseradish peroxidase-labeled streptavidin solution (1:500) and incubated for 30 min. Finally, the samples were developed using the diaminobenzidine substrate, chromogen, H_2O_2, and diaminobenzidine for 10 min. The samples were washed and examined under light microscope (200×). The counting was repeated three times, and the percentage from each counting was calculated.

Immunoblot Analysis. Cell lysates were prepared according to methods published previously (Kang et al., 2003). In brief, the cells were centrifuged at 3000*g* for 3 min and allowed to expand osmotically to the point of lysis after the addition of lysis buffer. Lysates were centrifuged at 10,000*g* for 10 min to obtain supernatants and stored at −70°C until use. Immunoblot analysis was performed

according to the procedures published previously (Bae et al., 2007). Protein bands of interest were developed using the ECL chemiluminescence system (Amersham, Chalfont St. Giles, Buckinghamshire, UK). Equal loading of protein was verified by immunoblotting for β-actin.

Flow Cytometric Analysis of Mitochondrial Membrane Potential. Mitochondrial membrane potential (MMP) was measured with Rh123, a membrane-permeable cationic fluorescent dye. The cells were treated as specified, stained with 0.05 μg/ml Rh123 for 1 h, and harvested by trypsinization. After washing with PBS containing 1% fetal bovine serum, the cells were stained with 0.25 μg of PI. The change in MMP was monitored using a BD FACSCalibur flow cytometer (BD Biosciences, San Jose, CA). In each analysis, 15,000 events were recorded.

Measurement of ROS. DCFH-DA is a cell-permeable nonfluorescent probe that is cleaved by intracellular esterases and turns into the fluorescent dichlorofluorescein upon reaction with ROS. The level of ROS generation was determined by the concomitant increase in dichlorofluorescein fluorescence. After treatments, the cells were stained with 20 μM DCFH-DA for 1 h at 37°C. The fluorescence intensity in the cells was measured using a BD FACSCalibur flow cytometer (BD Biosciences). In each analysis, 10,000 events were recorded.

Measurement of Mitochondrial ROS. MitoSOX is a live cell-permeable and mitochondrial localizing superoxide indicator. After treatment of HepG2 cells with AA + iron, the cells were stained with 5 μM MitoSOX for 10 min at 37°C. The fluorescence intensity in the cells was measured using a BD FACSCalibur flow cytometer (BD Biosciences). In each analysis, 10,000 events were recorded.

Data Analysis. Scanning densitometry was performed with Image Scan and Analysis System (Alpha-Innotech Corporation, San Leandro, CA). One-way analysis of variance procedures were used to assess significant differences among treatment groups. For each treatment showing statistically significant effect, the Newman-Keuls test was used for comparisons of multiple group means. The criterion for statistical significance was set at $p < 0.05$ or $p < 0.01$.

Results

Induction of Cell Death and Mitochondrial Dysfunction by AA. To assess whether AA alters cell viability, an MTT assay was conducted on cells treated with various concentrations of AA for 12 h. AA significantly induced cell death at 10 or 30 μM (Fig. 1A). In each of the subsequent experiments, 10 μM AA was used. Light microscopic analysis confirmed the apoptotic morphological changes of cells treated with AA. The effect of AA on cell viability was confirmed by TUNEL assay. The number of TUNEL-positive cells was significantly increased after AA treatment for 12 h (Fig. 1B). To verify the induction of apoptosis by AA, cell lysates were immunoblotted for marker proteins associated with apoptosis (Fig. 1C). AA treatment caused PARP cleavage, procaspase-3 activation (shown as a decrease in the level of procaspase-3), and decreased the level of Bcl-x_L, all of which confirmed apoptosis.

Previous studies have shown that AA causes impairment of mitochondrial respiratory activity, thereby inducing mitochondrial dysfunction (Cocco et al., 1999). In an attempt to correlate AA-induced apoptosis with an alteration in mitochondrial function, MMP was measured using FACS after staining cells with Rh123 and PI. AA treatment (12 h) significantly increased the subpopulation of Rh123-negative and PI-negative cells (bottom left quadrant), which represents viable cells with mitochondrial damage (Fig. 1D). As expected, the fraction of apoptotic cells in the Rh123-negative and PI-positive field (top left quadrant) also increased. These results provide evidence that AA treatment induces apoptosis and mitochondrial dysfunction.

Iron Enhancement of AA-Induced Cell Death. Given previous observations showing that excess iron accumulation is a progressive factor in certain diseases such as hepatitis and liver fibrosis (George et al., 1998) and that excess ROS production catalyzed by iron enhanced toxicant-induced cell death (Kumar et al., 2005), an assessment of whether iron potentiates AA-induced apoptosis and ROS production was performed. Light microscopic analysis of cells treated with AA + iron showed the morphological changes of apoptotic cell death (Fig. 2A, top). The MTT assays confirmed that iron treatment alone moderately decreased cell viability, whereas the combinatorial treatment of AA with iron markedly decreased it (Fig. 2A, middle). As the concentration of AA was increased, the extent of cell death induced by iron (5 μM) was greatly enhanced (Fig. 2A, bottom). Moreover, treatment of AA and iron notably increased ROS production compared with AA or iron treatment alone (Fig. 2B).

Next, the effects of PEG-SOD (300 U/ml) and PEG-catalase (1000 U/ml) on ROS production were examined in cells exposed to AA + iron. Either PEG-SOD or PEG-catalase treatment notably or completely attenuated the ROS production, indicating that oxidant species such as superoxide and hydrogen peroxide might be involved in the process (Fig. 2C). Moreover, Trolox (100 μM, 19 h) or NAC (2 mM, 19 h) treatment enabled cells to survive against AA + iron, further supporting the notion that excess ROS causes cell death (Fig. 2D). These results demonstrate that iron enhances AA-induced cell death, which results from excess production of ROS.

Mitochondrial ROS Production and Dysfunction by AA + Iron. Next, mitochondrial ROS production was analyzed using MitoSOX, a live cell-permeable and mitochondrial localizing superoxide indicator. AA + iron treatment markedly increased the mitochondrial MitoSOX fluorescence (Fig. 3A), providing convincing evidence that AA + iron treatment promotes mitochondrial ROS production. Moreover, simultaneous iron treatment (5 μM) increased mitochondrial damage induced by AA (10 μM). The increase in the Rh123-negative cell subpopulation seemed to be greater in cells treated with AA + iron than those treated with AA alone (36 versus 23%) (Fig. 3B).

Studies have demonstrated that cyclosporin A, an inhibitor of permeability transition pore formation, prevents AA-induced mitochondrial dysfunction (Petronilliet al., 2001; Scorrano et al., 2001). To address whether loss in MMP is upstream of apoptosis in this model, additional experiments were carried out with cyclosporin A. Cyclosporin A treatment (2.5 μg/ml, 19 h) significantly inhibited AA + iron-induced cell death (Fig. 3C), supporting the role of a change in MMP in apoptosis induced by AA + iron.

Oltipraz Inhibition of Mitochondrial Dysfunction Induced by AA + Iron. Oltipraz induces phase II enzymes in vitro and in vivo and increases glucose use against TNFα or sorbitol (Wang et al., 1999; Kang et al., 2003; Bae et al., 2007, 2008). In this study, the capacity of oltipraz to restore MMP in cells exposed to AA + iron was examined. Oltipraz was effective in abolishing mitochondrial dysfunction induced by AA or enhanced mitochondrial dysfunction induced by AA + iron (Fig. 4A). These results corroborate the inhibitory effect

of oltipraz on the detrimental changes in MMP and support the notion that the cytoprotective effect of oltipraz may result from the restoration of mitochondrial function.

AA directly inhibits complexes I and III in the respiratory chain of mitochondria (Cocco et al., 1999). In an additional experiment, oltipraz was found to attenuate apoptosis induced by rotenone (complex I inhibitor) but not that by antimycin A (complex III inhibitor) (Fig. 4B), suggesting that the inhibition of AA-induced apoptosis by oltipraz might be associated with the electron transport system and that the target of oltipraz might reside in complex I or nearby sites.

Oltipraz Inhibition of Cell Death Induced by AA + Iron. In a subsequent experiment, we determined whether oltipraz inhibited apoptosis induced by AA + Iron. The MTT assay indicated that treatment of oltipraz at 3 μM significantly protected cells from injury induced by AA + Iron (Fig. 5A, left). A maximal cytoprotective effect was observed at 10 μM. A light microscopic morphological examination and TUNEL assay confirmed the protective effect of oltipraz against the challenge of AA + iron (Fig. 5, A and B). In addition, the levels of PARP, procaspase-3, and Bcl-x_L were decreased to greater extents in cells treated with AA + iron than in those treated with AA alone (Fig. 5C). The results of immunoblot analyses showing that oltipraz treatment prevented alterations in the levels of proteins associated with apoptosis verified its cytoprotective effect. A flow cytometric assay using DCFH-DA indicated that oltipraz treatment effectively attenuated ROS production increased by AA alone or AA + iron (Fig. 5D).

Inhibition of AA + Iron-Induced Mitochondrial Dysfunction by AMPK Activation. AMPK is an intracellular energy status sensor and is activated by cellular stresses, such as an increase in the AMP-to-ATP ratio. AMPK may also protect cells against mitochondrial dysfunction (Ido et al., 2002). The effects of AA with or without oltipraz on the timed responses of ACC and AMPK phosphorylations in HepG2 cells were examined. AA treatment increased the phosphorylation of ACC, which represents cellular AMPK activity (Fig. 6A). This was accompanied by an increase in

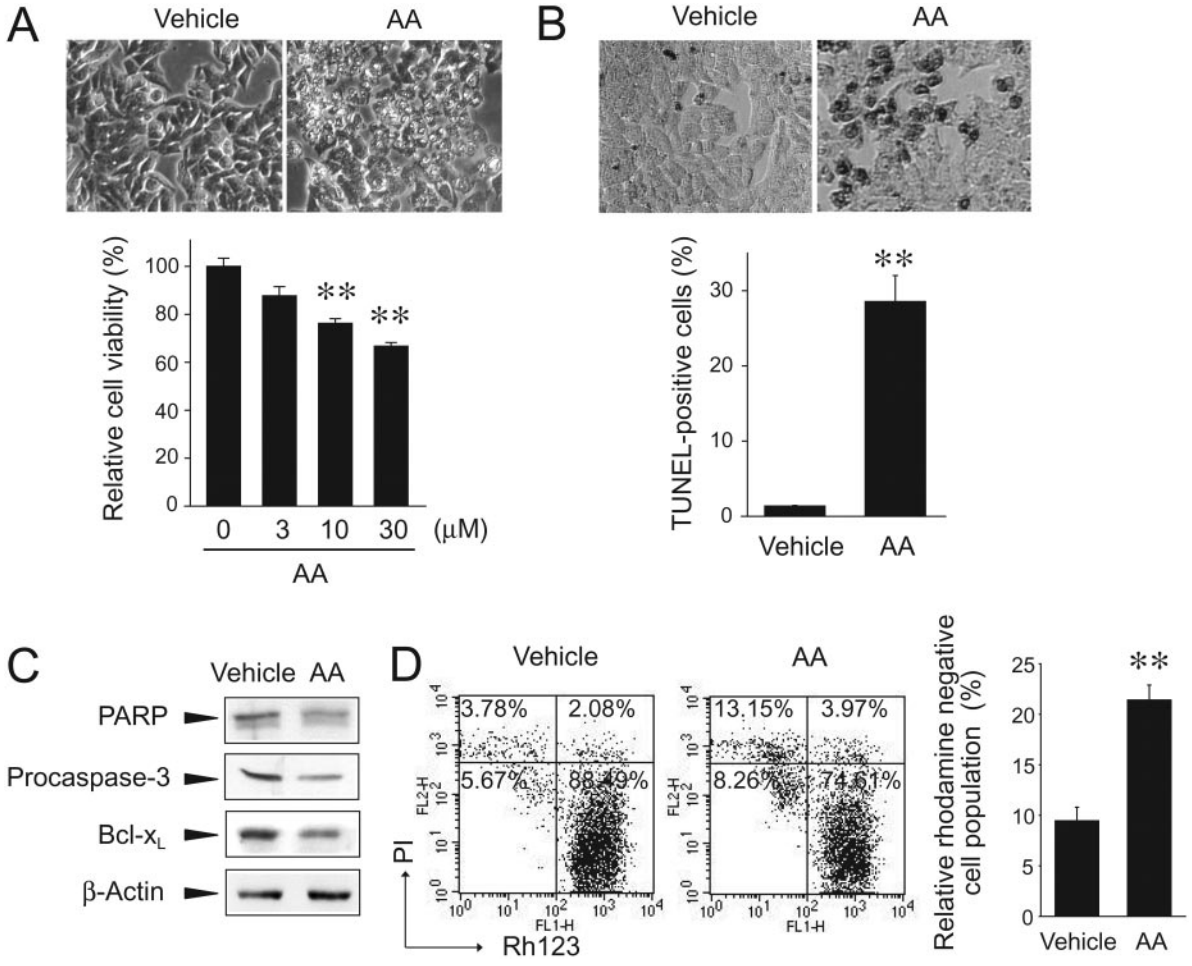

Fig. 1. Induction of apoptosis and mitochondrial dysfunction by AA. A, cell viability. Light microscopy shows the morphology of the cells treated with 10 μM AA for 12 h (magnification, 200×). The dose-response effect of AA on cell viability was assessed using MTT assays. Data represent the mean ± S.E. for four separate experiments (significant compared with vehicle-treated control; **, $p < 0.01$). B, TUNEL assays. Cells were treated with 10 μM AA for 12 h. The dark brown staining indicates positive TUNEL staining. The percentages of TUNEL-positive cells in HepG2 cells were quantified. Data represent the mean ± S.E. for three separate experiments (significant compared with vehicle-treated control, **$p < 0.01$). C, immunoblottings for proteins associated with apoptosis. Proteins were immunoblotted in cell lysates of HepG2 cells treated with 10 μM AA for 12 h. Results were confirmed by repeated experiments. D, MMP. HepG2 cells were treated as described above. After staining with Rh123, the cells were harvested and stained with PI. MMP was assessed by measuring the intensities of fluorescence from Rh123 and PI. Normal cells were located in the Rh123-positive and PI-negative field (bottom right), whereas viable cells with mitochondrial damage were in the Rh123-negative and PI-negative field (bottom left). Apoptotic cells were located in the Rh123-negative and PI-positive field (top left). Values represent the mean ± S.E. for three separate experiments (significant compared with vehicle-treated control, **, $p < 0.01$).

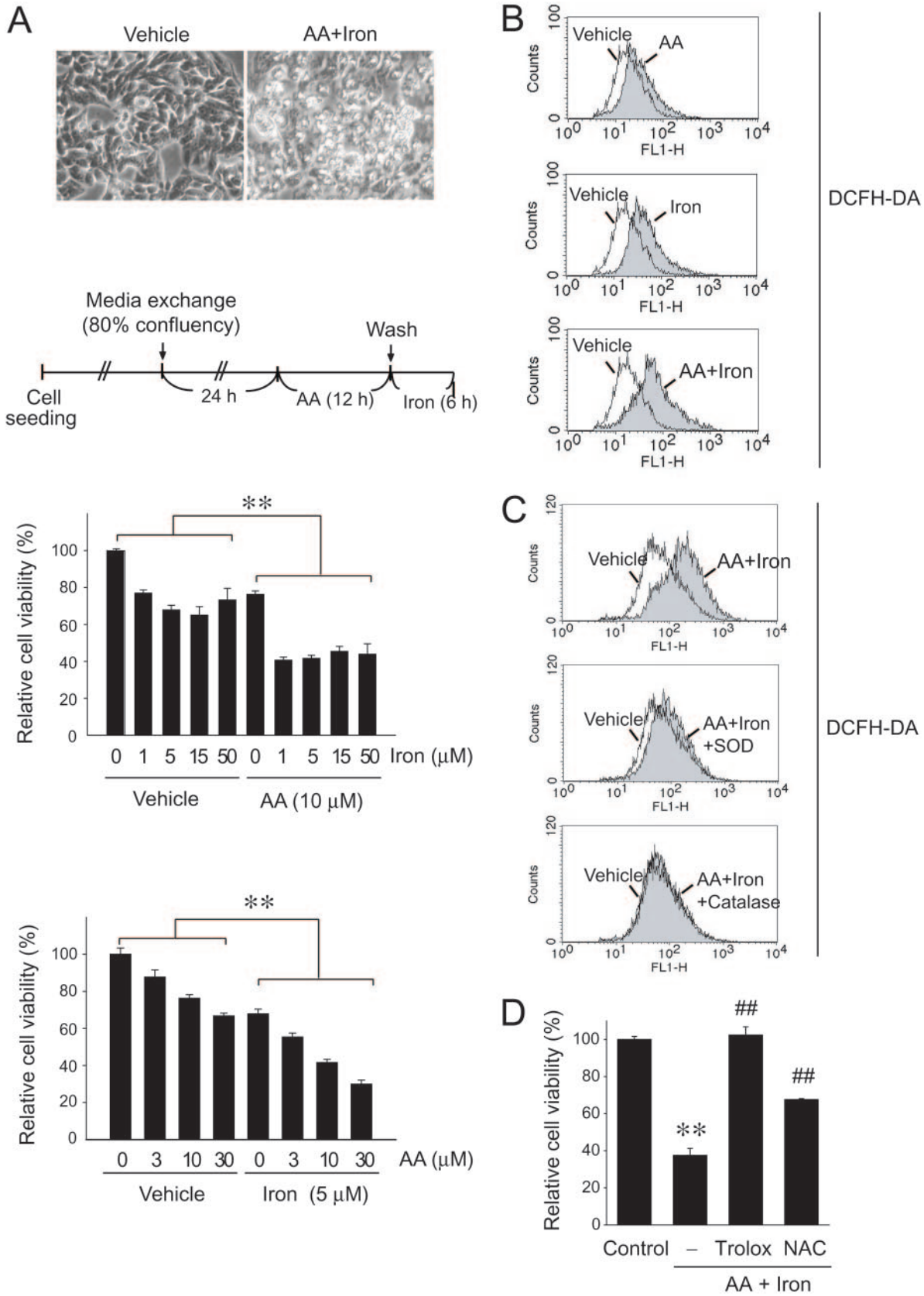

Fig. 2. Iron enhancement of cell death by AA. A, cell viability. Morphology (magnification, 200×) was examined in HepG2 cells that had been incubated with 10 μM AA for 12 h, washed with MEM, and then treated with 5 μM iron for 6 h (top). Cells were incubated with 10 μM AA for 12 h, washed with MEM, and then treated with various concentrations of iron for 6 h (middle). In separate experiments, cells were incubated with various concentrations of AA for 12 h and further exposed to 5 μM iron for 6 h (bottom). Cell viability was assessed by MTT assay. Data represent the mean ± S.E. for four separate experiments (significant compared with cells treated with AA or iron alone, **, $p < 0.01$). B, DCFH oxidation. DCFH oxidation was monitored

the phosphorylation of the AMPKα subunit, supporting the notion that oxidative stress caused by AA might stimulate AMPK. The increases in ACC and AMPK phosphorylations were greater in cells treated with both oltipraz and AA than in those treated with AA alone.

To assess the role of oltipraz's activation of AMPK in MMP transition and cell survival effects, we determined the effect of compound C, an inhibitor of AMPK, on rhodamine-negative cell subpopulations. Oltipraz treatment decreased the count of rhodamine-negative cells, which was reversed by simultaneous treatment of compound C (Fig. 6B). Moreover, the beneficial effects of oltipraz against MMP transition induced by AA or AA + iron were also antagonized by compound C, suggesting that oltipraz's activation of AMPK might contribute to the recovery of mitochondrial function. In another effort to verify the role of AMPK in the recovery of mitochondrial function, we determined the effect of AICAR, a chemical activator of AMPK, on the MMP transition (Fig. 6C). AICAR treatment (500 or 1000 μM) attenuated the AA- or AA + iron-induced increases in rhodamine-negative cell populations. These results provide evidence that the cytoprotective effect and the recovery of mitochondrial function by oltipraz might be associated at least in part with the activation of AMPK.

Inhibition of DCFH Oxidation and Mitochondrial Dysfunction by Dithiolethione Congeners. Given the current finding that oltipraz increased cell viability through an AMPK-dependent recovery of mitochondrial function, novel 1,2-dithiole-3-thione analogs that activate AMPK (Bae et al., 2007) were used in an effort to find additional compounds capable of protecting cells from oxidative injury (Fig. 7A). All of the new synthetic 1,2-dithiole-3-thione compounds with the capability of AMPK activation (i.e., CJ 11764, CJ11766, CJ11788, CJ11792, CJ11840, CJ11842, CJ12064, and CJ12073; 30 μM each) significantly inhibited ROS production promoted by AA + iron (Fig. 7B). To confirm their functional effectiveness, the effects of these compounds on the rhodamine-negative cell subpopulation were examined. All of the new 1,2-dithiole-3-thiones showed inhibition of MMP transition induced by AA + iron comparable with that

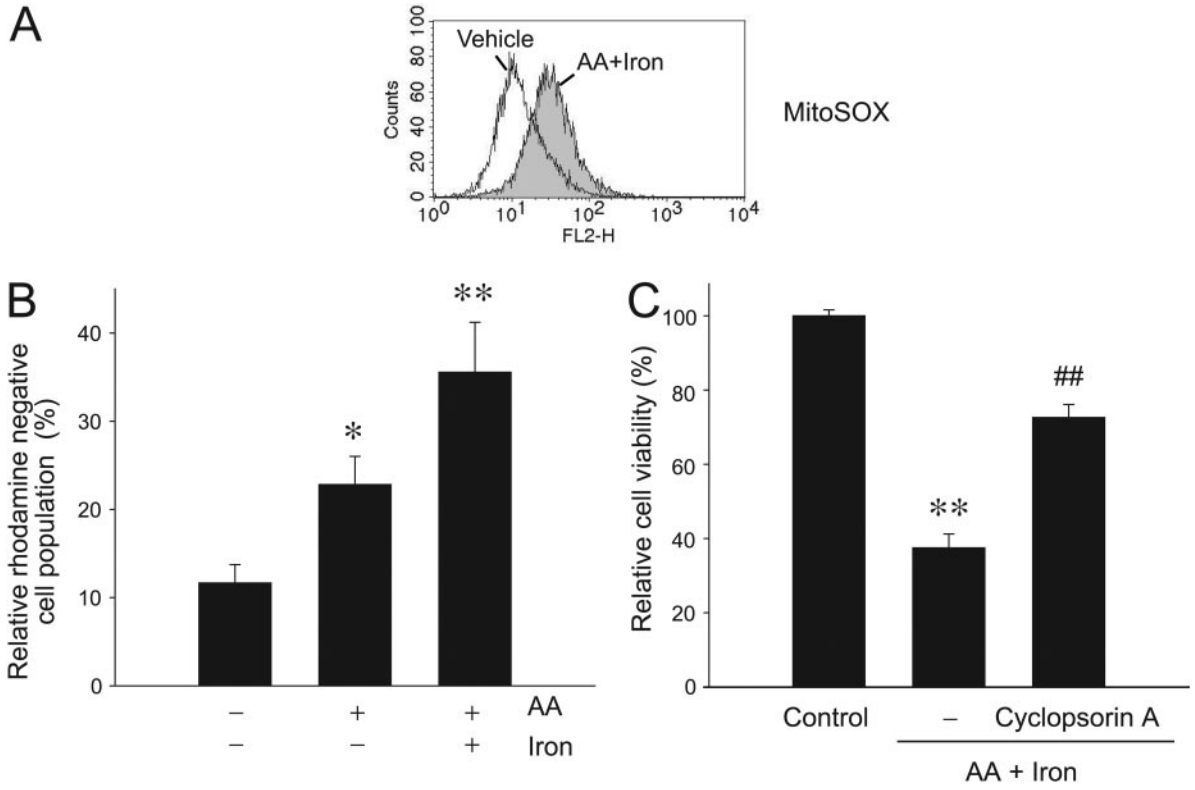

Fig. 3. The role of mitochondrial dysfunction in cell death induced by AA + iron. A, ROS production in mitochondria. Cells were treated with 10 μM AA (12 h) followed by additional incubation with 5 μM iron (1 h) and then stained with MitoSOX. Increase in MitoSOX fluorescence indicates the production of mitochondrial ROS in cells treated with AA + iron. B, Rh123-negative cell subpopulation. Cells were treated with 10 μM AA (12 h) alone or followed by additional incubation with 5 μM iron (1 h) and stained with Rh123 and PI. Data represent the mean ± S.E. for four separate experiments (significant compared with vehicle-treated control, *, $p < 0.05$, **, $p < 0.01$) C, MTT assay. Cells were incubated with 2.5 μg/ml cyclosporin A, followed by the addition of 10 μM AA for 12 h, washed with MEM, and finally treated with 5 μM iron for 6 h (significant compared with vehicle-treated control, **, $p < 0.01$; significant compared with cells treated with AA + iron, ##, $p < 0.01$).

in cells treated with AA (10 μM, 12 h), iron (5 μM, 1 h), or AA + iron (10 μM AA for 12 h followed by additional incubation with 5 μM iron for 1 h). The combinatorial treatment of AA + iron increased ROS production to a greater extent than the individual treatment, as evidenced by a larger increase in DCF fluorescence. C, the effects of SOD and catalase on DCFH oxidation. Cells were incubated with either PEG-SOD (300 U/ml) or PEG-catalase (1000 U/ml) for 1 h, followed by the addition of 10 μM AA for 12 h, washed with MEM, and finally treated with 5 μM iron for 1 h. Either PEG-SOD or PEG-catalase treatment prevented the ability of AA + iron to increase DCF fluorescence. D, increase in cell viability by antioxidants. Cells were incubated with 100 μM Trolox or 2 mM NAC for 1 h, followed by the addition of 10 μM AA for 12 h, washed with MEM, and finally treated with 5 μM iron for 6 h. Data represent the mean ± S.E. for four separate experiments (significant compared with vehicle-treated control, **, $p < 0.01$; significant compared with cells treated with AA + iron, ##, $p < 0.01$).

of oltipraz (Fig. 7C). Together, these results demonstrate that oltipraz or novel 1,2-dithiole-3-thione congeners with the ability to activate AMPK enable cells to efficaciously suppress ROS production and changes in mitochondrial permeability transition.

Discussion

Proinflammatory lipids play important roles in the development of diseases such as hepatitis. Among polyunsaturated fatty acids, AA serves as an inflammatory mediator in several organs and systems. It is known that the human plasma levels of nonesterified AA vary from 5.8 to 49 μM (Corey and Rosoff, 1991; Pompeia et al., 2003). However, the available plasma AA concentration is lower than 0.1 μM because of the presence of albumin (Brash, 2001). More importantly, inflammation increases AA levels in microenvironments, in which concentrations may reach ~100 μM (Brash, 2001; Pompeia et al., 2003). Therefore, the 10 μM AA treatments used in this study are within an achievable range. Studies have shown that AA has a direct effect on mitochondria: the mitochondrial permeability transition opened by AA leads to a loss of MMP and release of cytochrome *c* (Scorrano et al., 2001; Maia et al., 2006). In particular, AA impairs mitochondrial respiratory activity by selectively inhibiting complex I and III (Cocco et al., 1999). Here, we verify that AA treatment increased both mitochondrial injury and apoptosis, as supported by the induction of PARP and caspase-3 cleavage, and decrease in Bcl-x_L.

Iron promotes excess oxidant production and lipid peroxidation (Kumar and Bandyopadhyay, 2005). In the present study, we confirm that AA + iron catalyzes the overproduction of ROS and induces mitochondrial dysfunction and cell death. The function of mitochondria, a key intracellular organelle in healthy cellular function, has been extensively studied because mitochondrial dysfunction ultimately leads to pathogenesis regardless of its initial cause (Browning and Horton, 2004). The mitochondrial respiratory chain is one of the main sites of ROS production (Browning and Horton,

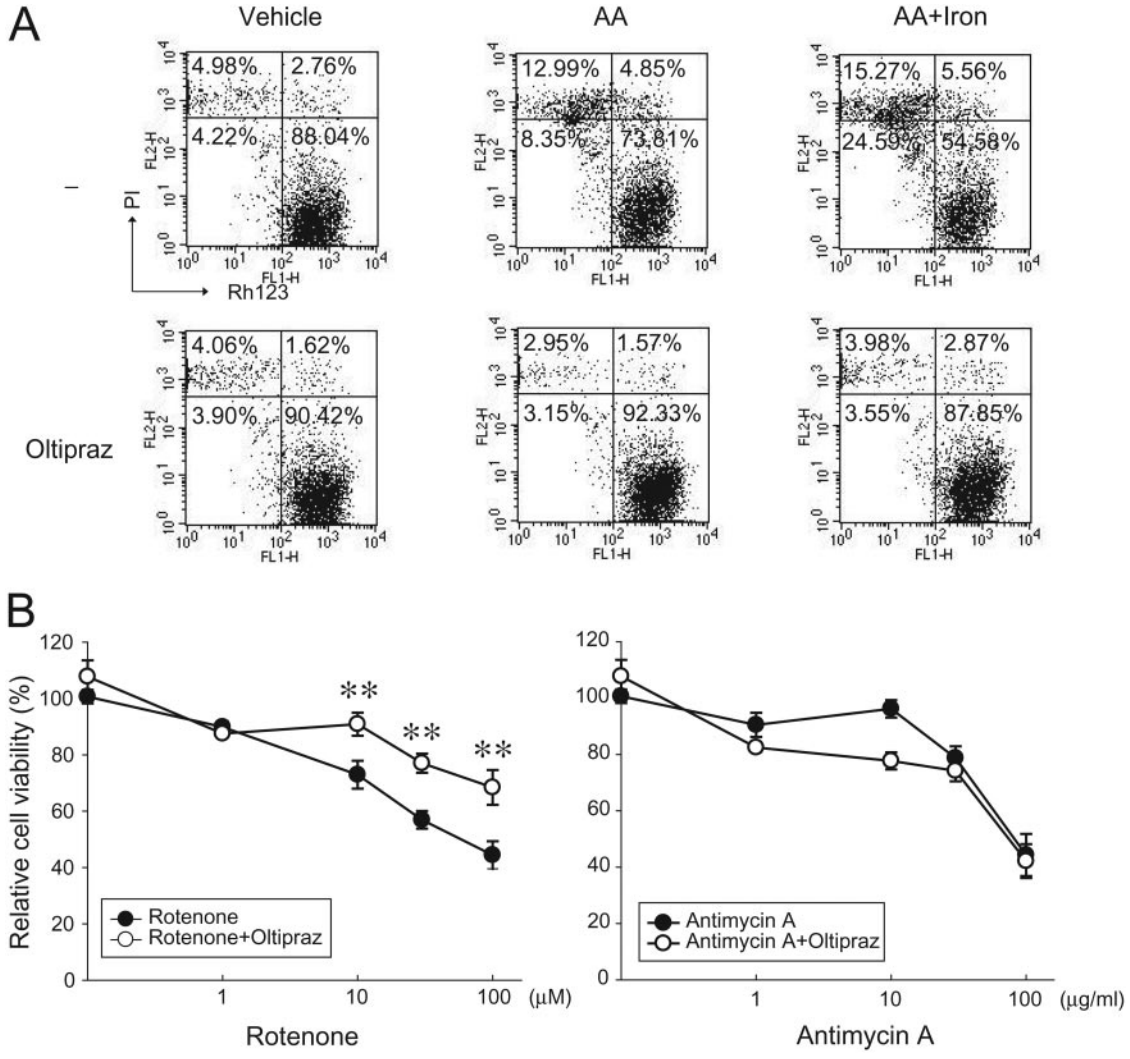

Fig. 4. Oltipraz inhibition of mitochondrial dysfunction induced by AA + iron. A, changes in MMP. Cells were treated with 10 μM oltipraz for 30 min, followed by the addition of AA (10 μM) or AA + iron (5 μM). AA or AA + iron treatment significantly increased the subpopulation of Rh123-negative and PI-negative cells (bottom left quadrant), which represents viable cells with mitochondrial damage, and the fraction of apoptotic cells in the Rh123-negative and PI-positive field (top left quadrant). Oltipraz treatment abolished mitochondrial dysfunction induced by AA or AA + iron. B, MTT assay. Cells were incubated with oltipraz, followed by the addition of various concentrations of rotenone (1–100 μM) or antimycin A (1–100 μg/ml) for 24 h (significant compared with cells treated with rotenone, **, $p < 0.01$).

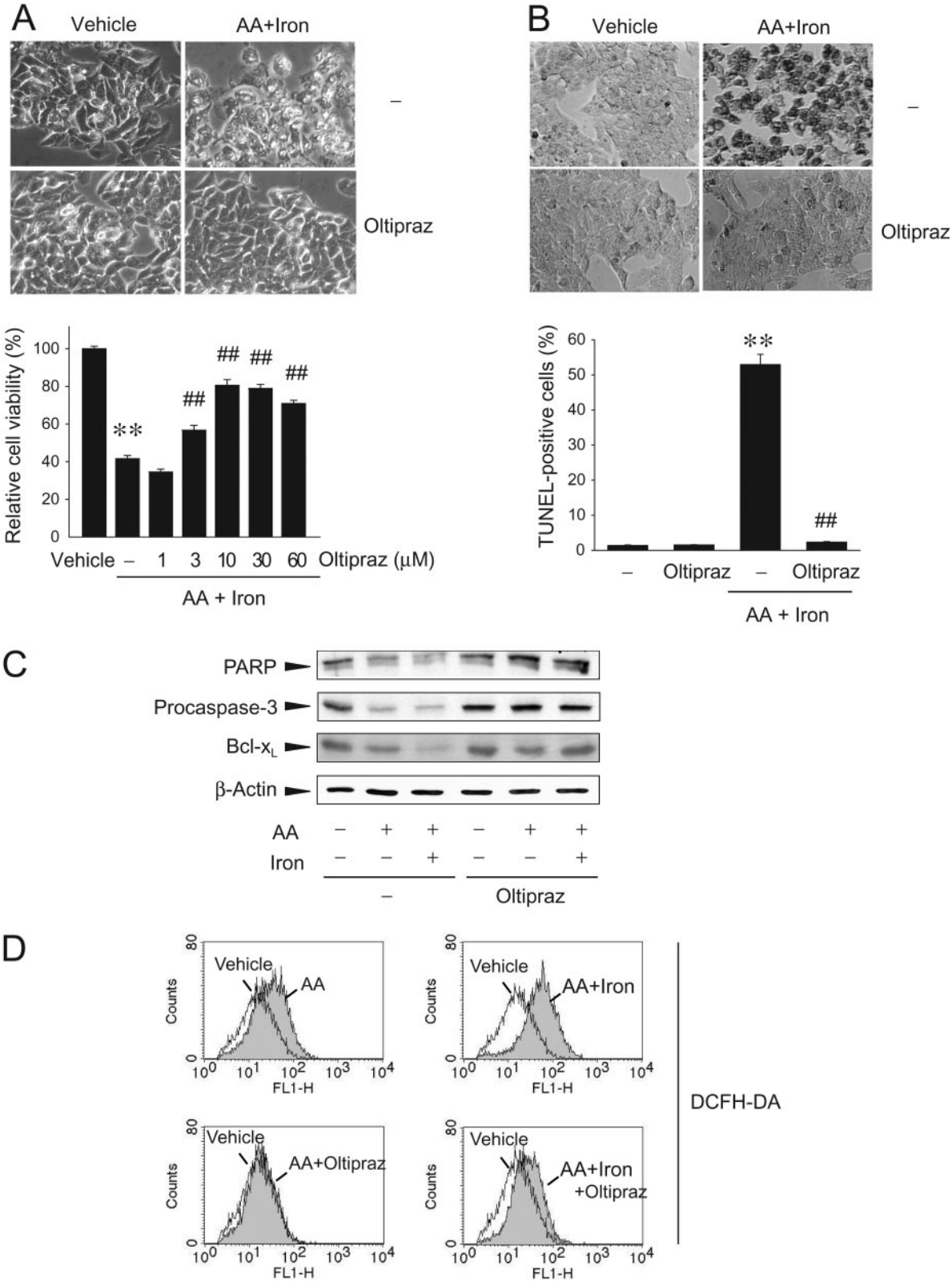

Fig. 5. Oltipraz inhibition of cell death induced by AA + iron. A, the effect of oltipraz on cell viability. Cells were incubated with 10 μM oltipraz for 30 min, followed by the addition of 10 μM AA for 12 h, washed with MEM, and finally treated with 5 μM iron for 6 h (top, magnification, 200×). The dose response effect of oltipraz on cell viability was assessed by MTT assays (bottom). Data represent the mean ± S.E. for four separate experiments (significant compared with vehicle-treated control, **, $p < 0.01$; significant compared with cells treated with AA + iron, ##, $p < 0.01$). B, TUNEL assay. Cells were treated with 10 μM oltipraz for 30 min, followed by the addition of 10 μM AA for 12 h, washed with MEM, and finally treated with 5 μM iron for 6 h. The percentages of TUNEL-positive cells (dark brown staining) were quantified. Data represent the mean ± S.E. for four separate experiments (significant compared with vehicle-treated control, **, $p < 0.01$; significant compared with cells treated with AA + iron, ##, $p < 0.01$). C, immunoblottings for apoptotic marker proteins. Proteins were immunoblotted in cell lysates. Results were confirmed by four separate experiments. D, DCFH oxidation. Cells were incubated with oltipraz for 30 min, followed by the addition of AA or AA + iron. Results were confirmed by repeated experiments. Oltipraz treatment attenuated AA- or AA + iron-induced ROS production, as evidenced by the decrease in DCF fluorescence.

2004). We demonstrate by PEG-SOD, PEG-catalase, Trolox, and NAC experiments that mitochondria play a key role in excess ROS production in cells treated with AA + iron. The data showing the inhibition of MMP transition by cyclosporin A further supports the hypothesis that AA + iron-induced apoptosis might be due to mitochondrial injury and the resultant overproduction of ROS. Moreover, our experiment using MitoSOX clearly identifies mitochondrial ROS production by AA + iron. The concept that mitochondrial ROS plays a crucial role in the process of apoptosis has been generally accepted. This contention is supported by our observation that AA + iron greatly promotes apoptosis along with mitochondrial dysfunction and ROS production. In the amplification steps, ROS generated in a lipid-rich environment would promote the induction of lipid peroxidation, thereby releasing highly reactive aldehyde derivatives. We found that apocynin, but not diphenyleneiodonium chloride, protects cells against AA + iron, which suggests that NADPH oxidase might also contribute to cell death induced by AA + iron. The lack of protection by diphenyleneiodonium chloride may be due to its inhibition of mitochondrial respiratory complex I and to NADPH oxidase (Holland et al., 1973).

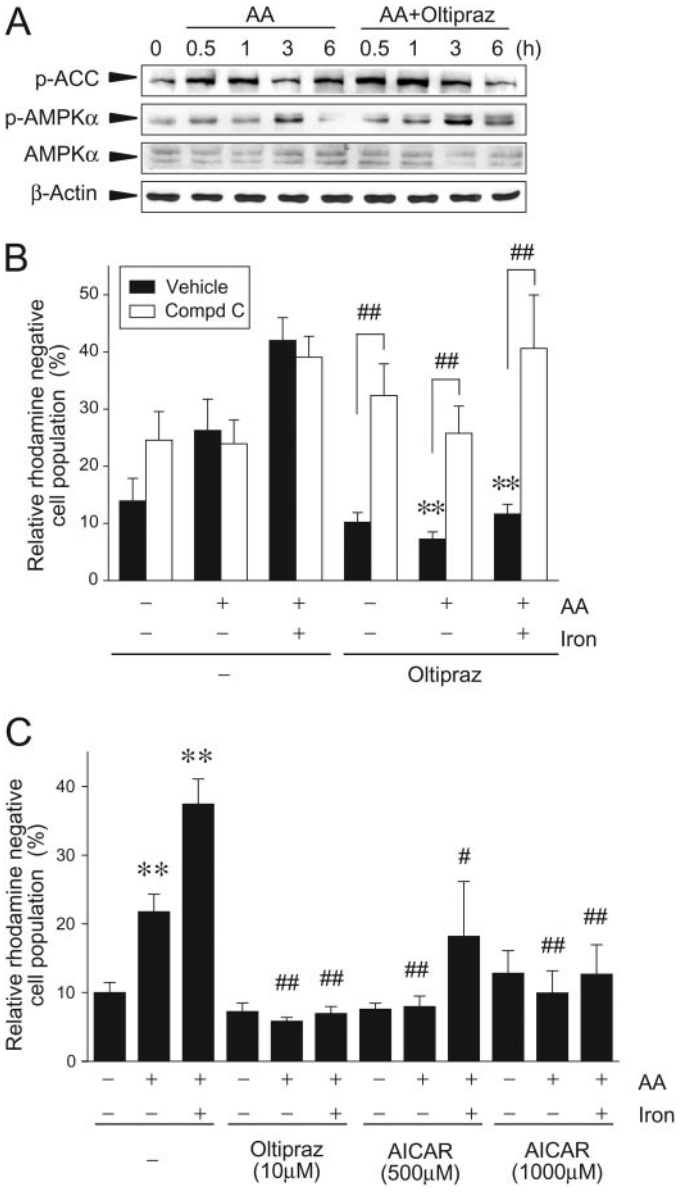

Fig. 6. The role of AMPK activation by oltipraz in MMP. A, AMPK activation. Immunoblot analyses were performed on cell lysates from cultures treated with AA alone or in combination with oltipraz for the indicated time periods. B, compound C-induced reversal of oltipraz's restoration of MMP. After treatment of compound C (3 μM, 30 min), cells were incubated with oltipraz for 30 min followed by the addition of AA or AA + iron. Data represent the mean ± S.E. for four separate experiments (significant compared with respective vehicle-treated control, **, $p < 0.01$; significant compared with respective treatment, ##, $p < 0.01$). C, MMP restoration by AICAR. Cells were incubated with AICAR for 30 min followed by the addition of AA or AA + iron. Data represent the mean ± S.E. for four separate experiments (significant compared with vehicle-treated control, **, $p < 0.01$; significant compared with respective AA or AA + iron treatment in control cells, #, $p < 0.05$, ##, $p < 0.01$).

In a previous study, oltipraz and other dithiolethiones directly increased ROS production in vitro (Kim and Gates, 1997) probably because conjugation of dithiolethione with cellular thiols enhances conversion of molecular oxygen to ROS. However, oltipraz exerts antioxidant effects in the liver as a consequence of Nrf2 and CCAAT/enhancer binding protein β-mediated induction of phase II enzymes (Kang et al., 2003). Our results show that oltipraz treatment effectively inhibits mitochondrial permeability transition by AA + iron. In addition, oltipraz and 1,2-dithiole-3-thione congeners were capable of inhibiting AA + iron-induced ROS production, thereby protecting cells from ROS-induced apoptosis. It is worth noting that oltipraz shows a cytoprotective effect at the concentration of 3 μM (Fig. 5), which is much lower than those of direct scavengers (Trolox, 100 μM; and NAC, 2 mM), implying that the antioxidant effects of oltipraz and congeners might result from cellular response, but not direct scavenging of ROS. Our observation that oltipraz attenuates apoptosis induced by rotenone, but not that by antimycin A suggests that oltipraz inhibition of apoptosis might be associated with complex I or nearby sites. All of these data support the concept that these compounds protect cells from excess ROS production through the recovery of mitochondrial function.

Oltipraz and 1,2-dithiole-3-thione derivatives prevent hepatic insulin resistance, which might be associated with endoplasmic reticulum (ER) stress (Xue et al., 2005; Bae et al., 2007). It is well recognized that impaired mitochondrial function may cause ER stress (Xu et al., 2004). The effect of oltipraz was additionally determined in cells treated with AA alone. Oltipraz decreased AA-induced ER expansion, as evidenced by a reduced shift to the right of the fluorescence of brefeldin A-BODIPY in the treated cell population (data not shown). Complete prevention of the increases in CCAAT enhancer-binding protein homologous protein (CHOP), glucose-regulated protein 78 (Grp78), and glucose-regulated protein 94 mRNA levels confirmed the inhibitory effect of oltipraz against AA-induced ER stress (data not shown). However, AA failed to induce XBP1 splicing, whereas thapsigargin [an inhibitor of sarco(endo)plasmic reticulum Ca^{2+} ATPase in ER] treatment promoted XBP1 splicing. Therefore, AA might induce ER stress in an XBP1-independent manner. In contrast, oltipraz treatment failed to reduce increases in *CHOP* and *Grp78* mRNA induced by thapsigargin. The results showed that oltipraz might inhibit ER stress induced by AA probably as a consequence of its inhibitory effect on mitochondrial dysfunction.

AMPK serves as a key regulator of cell survival or death in response to stressful situations. We found that AMPK activation by oltipraz protects cells from AA-induced apoptosis

and restores MMP. In this model, the cell survival effect of oltipraz depends on mitochondrial function via AMPK. The protective effects of oltipraz on MMP transition induced by AA or AA + iron were reversed by compound C. In addition AMPK activator similarly protected cells from mitochondrial injury. Moreover, we found that compound C treatment alone induces MMP transition, indicating that the constitutive activity of AMPK might be required for MMP regulation.

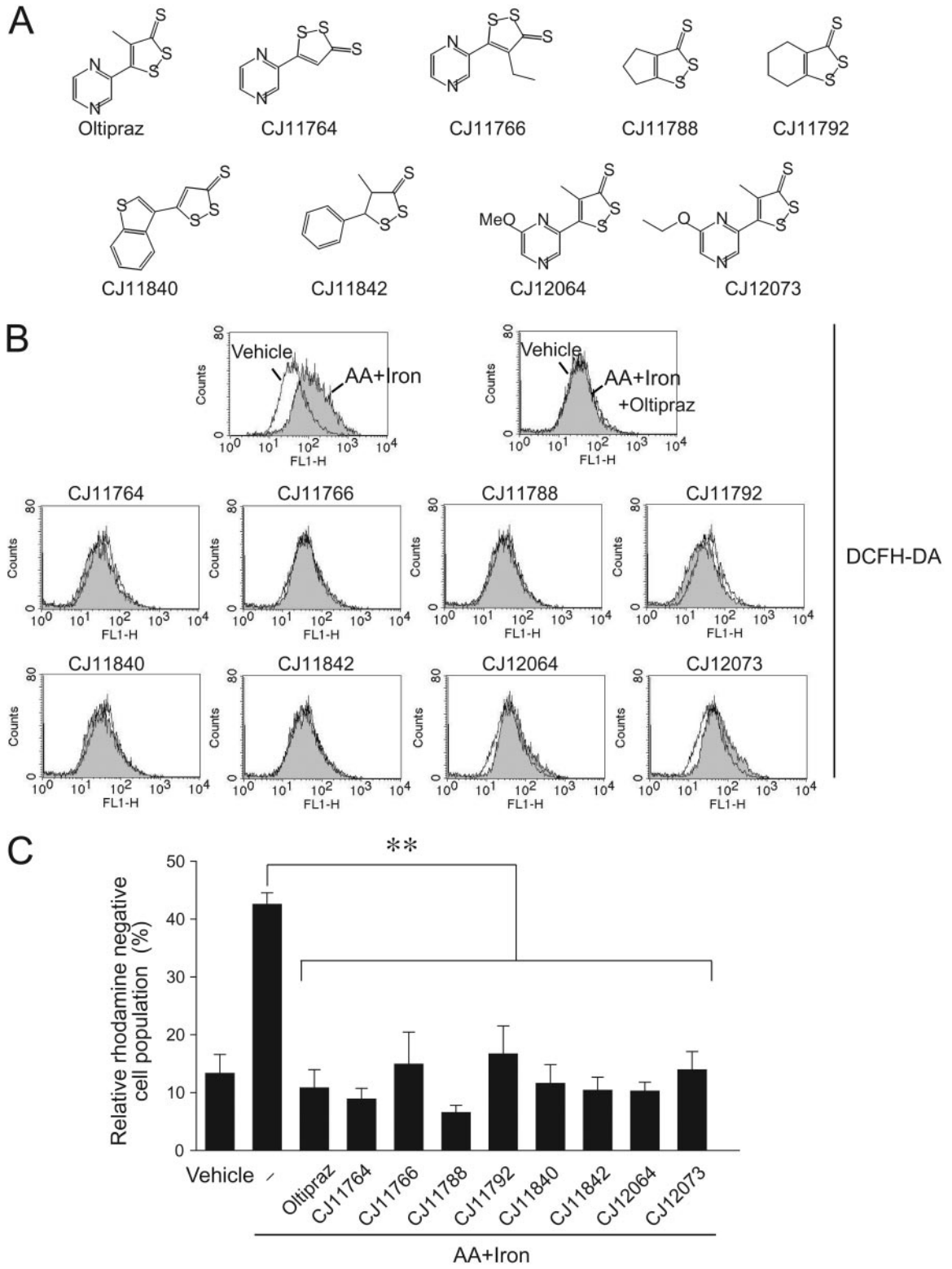

Fig. 7. The effects of 1,2-dithiole-3-thione congeners on DCFH oxidation and mitochondrial function. A, bond-line chemical structures of novel 1,2-dithiole-3-thiones. B, inhibition of DCFH oxidation. C, restoration of MMP. Cells were incubated with 30 μM concentration of each compound followed by the addition of AA + iron. Data represent the mean ± S.E. for four separate experiments (significant compared with cells treated with AA + iron, **, $p < 0.01$).

Furthermore, other 1,2-dithiole-3-thiones with the ability to activate AMPK also efficaciously inhibit AA-induced mitochondrial dysfunction, supporting our conclusion that the novel class of 1,2-dithiole-3-thiones has the ability to protect cells from mitochondrial oxidative stress via AMPK. Another study from this laboratory showed that oltipraz failed to directly activate AMPK in vitro (Bae et al., 2007). Therefore, the direct target of oltipraz seems to lie upstream of AMPK.

Oltipraz and other dithiolethiones activate AMPK, and their AMPK-dependent inhibition of p70 ribosomal S6 kinase-1 (S6K1) plays a key role in abolishing insulin resistance induced by TNFα (Bae et al., 2007). Insulin receptor substrate 1-mediated signaling is protected by 1,2-dithiole-3-thiones via S6K1 inhibition downstream of AMPK (Bae et al., 2007, 2008). However, we found that rapamycin, an inhibitor of mTOR-S6K1 activity that induces the dissociation of mTOR-raptor complex by binding FKBP12, has no effect in apoptosis induced by AA + iron (data not shown). Therefore, the cytoprotective effect of oltipraz in this model might not depend on the inhibition of S6K1. Glycogen synthase kinase-3β (GSK3β) inhibition contributed to the prevention of apoptosis in hepatocytes (Kim et al., 2005). However, we found that lithium chloride, a GSK3β inhibitor, had no effect in inhibiting apoptosis induced by AA + iron (data not shown). These results indicate that the cytoprotective effect of oltipraz might not solely depend on the inhibition of either S6K1 or GSK3β.

AMPK activation in certain physiological conditions might not be beneficial. Because AA increases oxidative stress and has a cytotoxic effect, AMPK activation by AA may reflect an adaptive response to toxic stress. Hyperosmolarity activates AMPK (Hayashi et al., 2000) as an adaptive response to external stress, resulting in cell shrinkage and the dissipation of mitochondrial transmembrane potential (Fumarola et al., 2005). In addition to the cytoprotective effect, we found that oltipraz and other dithiolethiones prevent hyperosmotic stress-induced hepatic insulin resistance through AMPK-dependent S6K1 inhibition (Bae et al., 2007). AICAR, an AMPK activator, inhibits cell injury induced by hypoxia, another AMPK-activating condition (Terai et al., 2005). Thus, the mechanistic basis of AMPK activation by AA may differ from that by oltipraz, which remains to be established.

In conclusion, oltipraz inhibits AA + iron-induced ROS production and protects MMP transition, thereby preventing cell death, which is mediated at least in part by AMPK activation. Oltipraz is a member of a novel class of dithiolethiones, many of which enable cells to prevent mitochondrial dysfunction induced by AA + iron. These findings show the potential of 1,2-dithiole-3-thiones to pharmacologically defend against excess oxidative stress through activation of the AMPK signaling pathway.

Acknowledgments

We are grateful to Dr. S. Carroll Brooks III for editing.

References

Araya J, Rodrigo R, Videla LA, Thielemann L, Orellana M, Pettinelli P, and Poniachik J (2004) Increase in long-chain polyunsaturated fatty acid n-6/n-3 ratio in relation to hepatic steatosis in patients with non-alcoholic fatty liver disease. *Clin Sci* **106:**635–643.

Bae EJ, Yang YM, Kim JW, and Kim SG (2007) Identification of a novel class of dithiolethiones that prevent hepatic insulin resistance via the adenosine monophosphate-activated protein kinase-p70 ribosomal S6 kinase-1 pathway. *Hepatology* **46:**730–739.

Bae EJ, Yang YM, and Kim SG (2008) Abrogation of hyperosmotic impairment of insulin signaling by a novel class of 1,2-dithiole-3-thiones through the inhibition of S6K1 activation. *Mol Pharmacol* **73:**1502–1512.

Balboa MA and Balsinde J (2006) Oxidative stress and arachidonic acid mobilization. *Biochim Biophys Acta* **1761:**385–391.

Bolton MG, Muñoz A, Jacobson LP, Groopman JD, Maxuitenko YY, Roebuck BD, and Kensler TW (1993) Transient intervention with oltipraz protects against aflatoxin-induced hepatic tumorigenesis. *Cancer Res* **53:**3499–3504.

Brash AR (2001) Arachidonic acid as a bioactive molecule. *J Clin Invest* **107:**1339–1345.

Browning JD and Horton JD (2004) Molecular mediators of hepatic steatosis and liver injury. *J Clin Invest* **114:**147–152.

Caro AA and Cederbaum AI (2001) Synergistic toxicity of iron and arachidonic acid in HepG2 cells overexpressing CYP2E1. *Mol Pharmacol* **60:**742–752.

Chang DJ, Ringold GM, and Heller RA (1992) Cell killing and induction of manganous superoxide dismutase by tumor necrosis factor-alpha is mediated by lipoxygenase metabolites of arachidonic acid. *Biochem Biophys Res Commun* **188:**538–546.

Cocco T, Di Paola M, Papa S, and Lorusso M (1999) Arachidonic acid interaction with the mitochondrial electron transport chain promotes reactive oxygen species generation. *Free Radic Biol Med* **27:**51–59.

Corey SJ and Rosoff PM (1991) Unsaturated fatty acids and lipoxygenase products regulate phagocytic NADPH oxidase activity by a nondetergent mechanism. *J Lab Clin Med* **118:**343–351.

Dwyer JH, Allayee H, Dwyer KM, Fan J, Wu H, Mar R, Lusis AJ, and Mehrabian M (2004) Arachidonate 5-lipoxygenase promoter genotype, dietary arachidonic acid, and atherosclerosis. *N Engl J Med* **350:**29–37.

Fumarola C, La Monica S, and Guidotti GG (2005) Amino acid signaling through the mammalian target of rapamycin (mTOR) pathway: role of glutamine and of cell shrinkage. *J Cell Physiol* **204:**155–165.

George DK, Goldwurm S, MacDonald GA, Cowley LL, Walker NI, Ward PJ, Jazwinska EC, and Powell LW (1998) Increased hepatic iron concentration in nonalcoholic steatohepatitis is associated with increased fibrosis. *Gastroenterology* **114:**311–318.

Hayashi T, Hirshman MF, Fujii N, Habinowski SA, Witters LA, and Goodyear LJ (2000) Metabolic stress and altered glucose transport: activation of AMP-activated protein kinase as a unifying coupling mechanism. *Diabetes* **49:**527–531.

Holland PC, Clark MG, Bloxham DP, and Lardy HA (1973) Mechanism of action of the hypoglycemic agent diphenyleneiodonium. *J Biol Chem* **248:**6050–6056.

Ido Y, Carling D, and Ruderman N (2002) Hyperglycemia-induced apoptosis in human umbilical vein endothelial cells: inhibition by the AMP-activated protein kinase activation. *Diabetes* **51:**159–167.

Jacobson LP, Zhang BC, Zhu YR, Wang JB, Wu Y, Zhang QN, Yu LY, Qian GS, Kuang SY, Li YF, et al. (1997) Oltipraz chemoprevention trial in Qidong, People's Republic of China: study design and clinical outcomes. *Cancer Epidemiol Biomarkers Prev* **6:**257–265.

Jayadev S, Linardic CM, and Hannun YA (1994) Identification of arachidonic acid as a mediator of sphingomyelin hydrolysis in response to tumor necrosis factor α. *J Biol Chem* **269:**5757–5763.

Kang KW, Cho IJ, Lee CH, and Kim SG (2003) Essential role of phosphatidylinositol 3-kinase-dependent CCAAT/enhancer binding protein beta activation in the induction of glutathione *S*-transferase by oltipraz. *J Natl Cancer Inst* **95:**53–66.

Kang KW, Kim YG, Cho MK, Bae SK, Kim CW, Lee MG, and Kim SG (2002) Oltipraz regenerates cirrhotic liver through CCAAT/enhancer binding protein-mediated stellate cell inactivation. *FASEB J* **16:**1988–1990.

Kensler TW (1997) Chemoprevention by inducers of carcinogen detoxication enzymes. *Environ Health Perspect* **105:**965–970.

Kim AJ, Shi Y, Austin RC, and Werstuck GH (2005) Valproate protects cells from ER stress-induced lipid accumulation and apoptosis by inhibiting glycogen synthase kinase-3. *J Cell Sci* **118:**89–99.

Kim W and Gates KS (1997) Evidence for thiol-dependent production of oxygen radicals by 4-methyl-5-pyrazinyl-3H-1,2-dithiole-3-thione (oltipraz) and 3H-1,2-dithiole-3-thione: possible relevance to the anticarcinogenic properties of 1,2-dithiole-3-thiones. *Chem Res Toxicol* **10:**296–301.

Kumar S and Bandyopadhyay U (2005) Free heme toxicity and its detoxification systems in human. *Toxicol Lett* **157:**175–188.

Maia RC, Culver CA, and Laster SM (2006) Evidence against calcium as a mediator of mitochondrial dysfunction during apoptosis induced by arachidonic acid and other free fatty acids. *J Immunol* **177:**6398–6404.

Mattera R, Stone GP, Bahhur N, and Kuryshev YA (2001) Increased release of arachidonic acid and eicosanoids in iron-overloaded cardiomyocytes. *Circulation* **103:**2395–2401.

Neale ML, Fiera RA, and Matthews N (1988) Involvement of phospholipase A2 activation in tumour cell killing by tumour necrosis factor. *Immunology* **64:**81–85.

Petronilli V, Penzo D, Scorrano L, Bernardi P, and Di Lisa F (2001) The mitochondrial permeability transition, release of cytochrome c and cell death. Correlation with the duration of pore openings in situ. *J Biol Chem* **276:**12030–12034.

Pompeia C, Lima T, and Curi R (2003) Arachidonic acid cytotoxicity: can arachidonic acid be a physiological mediator of cell death? *Cell Biochem Funct* **21:**97–104.

Sakurai K and Cederbaum AI (1998) Oxidative stress and cytotoxicity induced by ferric-nitrilotriacetate in HepG2 cells that express cytochrome P450 2E1. *Mol Pharmacol* **54:**1024–1035.

Scorrano L, Oakes SA, Opferman JT, Cheng EH, Sorcinelli MD, Pozzan T, and Korsmeyer SJ (2003) BAX and BAK regulation of endoplasmic reticulum Ca^{2+}: a control point for apoptosis. *Science* **300:**135–139.

Scorrano L, Penzo D, Petronilli V, Pagano F, and Bernardi P (2001) Arachidonic acid causes cell death through the mitochondrial permeability transition. Implications for tumor necrosis factor-α apoptotic signaling. *J Biol Chem* **276:**12035–12040.

Simopoulos AP (2006) Evolutionary aspects of diet, the omega-6/omega-3 ratio and genetic variation: nutritional implications for chronic diseases. *Biomed Pharmacother* **60:**502–507.

Tadolini B and Hakim G (1996) The mechanism of iron (III) stimulation of lipid peroxidation. *Free Radic Res* **25:**221–227.

Terai K, Hiramoto Y, Masaki M, Sugiyama S, Kuroda T, Hori M, Kawase I, and Hirota H (2005) AMP-activated protein kinase protects cardiomyocytes against hypoxic injury through attenuation of endoplasmic reticulum stress. *Mol Cell Biol* **25:**9554–9575.

Valerio LG Jr, Parks T, and Petersen DR (1996) Alcohol mediates increases in hepatic and serum nonheme iron stores in a rat model for alcohol-induced liver injury. *Alcohol Clin Exp Res* **20:**1352–1361.

Wang JS, Shen X, He X, Zhu YR, Zhang BC, Wang JB, Qian GS, Kuang SY, Zarba A, Egner PA, et al. (1999) Protective alterations in phase 1 and 2 metabolism of aflatoxin B1 by oltipraz in residents of Qidong, People's Republic of China. *J Natl Cancer Inst* **91:**347–354.

Xu W, Liu L, Charles IG, and Moncada S (2004) Nitric oxide induces coupling of mitochondrial signalling with the endoplasmic reticulum stress response. *Nat Cell Biol* **6:**1129–1134.

Xue X, Piao JH, Nakajima A, Sakon-Komazawa S, Kojima Y, Mori K, Yagita H, Okumura K, Harding H, and Nakano H (2005) Tumor necrosis factor α (TNFα) induces the unfolded protein response (UPR) in a reactive oxygen species (ROS)-dependent fashion, and the UPR counteracts ROS accumulation by TNFα. *J Biol Chem* **280:**33917–33925.

Address correspondence to: Dr. Sang Geon Kim, College of Pharmacy, Seoul National University, Sillim-dong, Kwanak-gu, Seoul 151-742, Korea. E-mail: sgk@snu.ac.kr